# Synthetic and Structural Studies on *trans*-Tetrapyridine Complexes of Ruthenium(II)

**Benjamin J. Coe,*,† Thomas J. Meyer,* and Peter S. White**

Department of Chemistry, The University of North Carolina, Chapel Hill, North Carolina 27599-3290

*Received July 21, 1994*[⊗]

The complexes *trans*-$Ru(NO_2)_2(py)_4$ (**1**) and *trans*-$Ru(CN)_2(py)_4$ (**2**) (py = pyridine) are prepared by reaction between *trans*-$RuCl_2(py)_4$ in refluxing aqueous pyridine and excess $NO_2^-$ or $CN^-$ respectively. The salt *trans*-$[RuCl(py)_4(NO)](PF_6)_2$ (**3**) is prepared from **1** by reflux in concentrated hydrochloric acid. Reaction of **3** with azide ion in acetone affords the labile intermediate *trans*-$[RuCl(py)_4(Me_2CO)]^+$. Subsequent reaction with nitrogen ligands, L, yields the derivatives *trans*-$[RuCl(py)_4(L)]^+$ which were isolated as their $PF_6^-$ salts (**4**, L = py; **5**, L = 4-ethylpyridine, 4-Etpy; **6**, L = benzonitrile, PhCN; **7**, L = pyrazine, pyz; **8**, L = 1-methylimidazole, 1-MeIm). The remaining chloride ligand is substituted in the presence of $TlPF_6$ at room temperature to afford the asymmetrical derivatives *trans*-$[Ru(py)_4(1\text{-MeIm})(MeCN)](PF_6)_2$ (**10**) from **8** and *trans*-$[Ru(py)_4(4\text{-Etpy})(dmabn)](PF_6)_2$ (**11**, dmabn = 4-(dimethylamino)benzonitrile) from **5**. The pyrazine-bridged salt $[\{trans\text{-}RuCl(py)_4\}_2(\mu\text{-pyz})](PF_6)_2$ (**9**) is prepared by reaction of *trans*-$[RuCl(py)_4(Me_2CO)]^+$ with either 1 equiv of **8** or with $^1/_2$ equiv of pyrazine. The single-crystal X-ray structures of *trans*-$[RuCl(py)_4(PhCN)]PF_6$ (**6**), *trans*-$[RuCl(py)_4(pyz)]PF_6$ (**7**), and **9** have been determined. The salt **6**, chemical formula $C_{27}H_{25}ClF_6N_5PRu$, crystallizes in the tetragonal space group *P4nc* with $a = 20.191(7)$ Å, $c = 14.557(7)$ Å, and $Z = 8$. **7**, chemical formula $C_{24}H_{24}ClF_6N_6PRu$, crystallizes in the tetragonal space group *P4/ncc* with $a = 10.7624(13)$ Å, $c = 24.615(3)$ Å, and $Z = 4$. The bimetallic salt $[\{trans\text{-}RuCl(py)_4\}_2(\mu\text{-pyz})](PF_6)_2\cdot 2DMF$ (**9**·2DMF), chemical formula $C_{50}H_{58}Cl_2F_{12}N_{12}O_2P_2Ru_2$, crystallizes in the monoclinic system, space group *C2/c* with $a = 19.0564(17)$ Å, $b = 14.664(3)$ Å, $c = 21.5112(22)$ Å, $\beta = 91.877(8)°$, and $Z = 4$.

## Introduction

Ruthenium polypyridyl complexes are the focus of much study, in part, because of their potential for incorporation into photochemical molecular devices.[1] The serious structural limitations imposed by the typical *cis* geometry of such complexes has caused us to investigate the possibility of preparing complexes having a *trans* structure. Some success was achieved by using complexes based upon the *trans*-$\{Ru(bpy)_2\}^{2+}$ center (bpy = 2,2′-bipyridine),[2] and a number of chromophore–quencher complexes have been synthesized and their photophysical properties investigated.[3] However, an inherent problem with these bpy-based systems is their poor thermal and photochemical stability. Hence we have begun to investigate other *trans* Ru centers as possible building blocks for the construction of photoactive molecular assemblies and selected the *trans*-$\{Ru(py)_4\}^{2+}$ center as a likely candidate. Although the $Ru^{II} \rightarrow$ py MLCT absorber is not a visible chromophore, the *trans*-$\{Ru(py)_4\}^{2+}$ center is highly stable and has the potential to act as a nonchromophoric spacer in mono- and oligometallic *trans* assemblies.

The complex *trans*-$[RuCl(py)_4(NO)]^{2+}$ was selected as a precursor because it contains two different axial ligands which might undergo stepwise substitution to afford asymmetric *trans* derivatives, a requirement for the construction of functionalized assemblies. Other workers have reported the preparation of *trans*-$[RuCl(py)_4(NO)]^{2+}$ as its $PF_6^-$ and $ClO_4^-$ salts from *trans*-$RuCl_2(py)_4$ via *trans*-$Ru(NO_2)_2(py)_4$.[4] It was found that the nitrosyl ligand in *trans*-$[RuCl(py)_4(NO)]^{2+}$ behaves as an electrophile in its reaction with azide ion at room temperature. Reaction of *trans*-$[RuCl(py)_4(NO)](ClO_4)_2$ with excess $N_3^-$ in aqueous ethanol produced a mixture of the complexes *trans*-$RuCl(N_3)(py)_4$ and *trans*-$[RuCl(py)_4(H_2O)]^+$ in low yield.[4] Reaction of *trans*-$[RuCl(py)_4(NO)](PF_6)_2$ with 1 equiv of $N_3^-$ in aqueous ethanol afforded the unstable complex *trans*-$[RuCl(py)_4(N_2)]^+$, also in low yield.[4] These results demonstrate that replacement of the nitrosyl ligand in *trans*-$[RuCl(py)_4(NO)]^{2+}$ is feasible under mild conditions. No attempts at substitution of the chloride ligand in either *trans*-$[RuCl(py)_4(NO)]^{2+}$ or in any of its derivatives have been reported.

## Experimental Section

**Materials and Procedures.** The complex *trans*-$RuCl_2(py)_4$ was prepared according to a previously published procedure.[5] All other reagents were obtained commercially and used as supplied. All reactions were conducted under an atmosphere of argon. Column chromatography was carried out by using silica gel 60 (70–230 mesh) with 5% (v/v) acetone/dichloromethane as eluent unless otherwise stated. Products were dried at room temperature in a vacuum desiccator for *ca.* 15 h prior to characterization.

**Physical Measurements.** $^1H$ NMR spectra were recorded on a Bruker AC200 spectrometer, and all shifts are referenced to TMS. In most cases, the signals for pyridine protons show fine splitting at this field, but are reported here as simple multiplets. IR spectra were obtained as KBr disks with a Mattson Galaxy Series FTIR 5000 instrument. UV–visible spectra were recorded by using a Hewlett Packard 8451A diode array spectrophotometer. Elemental analyses were performed by ORS, Whitesboro, NY. Cyclic voltammetric measurements were carried out by using a PAR Model 173 potentiostat with a PAR Model 175 universal programmer. A three-compartment cell was used with an SCE reference electrode separated from a Pt

† Present address: Department of Chemistry, The University of Manchester, Oxford Road, Manchester M13 9PL, U.K.

⊗ Abstract published in *Advance ACS Abstracts,* November 15, 1994.

(1) (a) Meyer, T. J. *Acc. Chem. Res.* **1989**, *22*, 163. (b) Balzani, V.; Scandola, F. *Supramolecular Photochemistry*; Ellis Horwood: Chichester, U.K., 1991, pp.123–151. (c) Mecklenburg, S. L.; Peek, B. M.; Schoonover, J. R.; McCafferty, D. G.; Wall, C. G.; Erickson, B. W.; Meyer, T. J. *J. Am. Chem. Soc.* **1993**, *115*, 5479, and refs therein.
(2) Coe, B. J.; Meyer, T. J.; White, P. S. *Inorg. Chem.* **1993**, *32*, 4012.
(3) Coe, B. J.; Friesen, D. A.; Thompson, D. W.; Meyer, T. J. Manuscript in preparation.
(4) Bottomley, F.; Mukaida, M. *J. Chem. Soc., Dalton Trans.* **1982**, 1933.
(5) Evans, I. P.; Spencer, A.; Wilkinson, G. *J. Chem. Soc., Dalton Trans.* **1973**, 204.

0020-1669/95/1334-0593$09.00/0 

**Table 1.** UV−Visible and Electrochemical Data in Acetonitrile

| complex (no.) | $E_{1/2}$, V vs SCE ($\Delta E_p$, mV)[a] Ru$^{III/II}$ | other waves | $\lambda_{max}$, nm ($\epsilon$, $M^{-1}$ $cm^{-1}$)[b] | assignment |
|---|---|---|---|---|
| *trans*-$RuCl_2(py)_4$ | 0.26 (80) | | 206 (29 000) | $\pi \rightarrow \pi^*$ |
| | | | 250 (15 700) | $\pi \rightarrow \pi^*$ |
| | | | 398 (25 100) | $d\pi \rightarrow \pi^*$ (py) |
| | | | 450 sh (7800) | $d\pi \rightarrow \pi^*$ |
| *trans*-$Ru(NO_2)_2(py)_4$ (**1**) | 0.90[c] | | 210 (26 800) | $\pi \rightarrow \pi^*$ |
| | | | 244 (14 300) | $\pi \rightarrow \pi^*$ |
| | | | 350 (19 000) | $d\pi \rightarrow \pi^*$ (py) |
| *trans*-$Ru(CN)_2(py)_4$ (**2**) | 0.80 (90) | | 204 (27 800) | $\pi \rightarrow \pi^*$ |
| | | | 248 (15 500) | $\pi \rightarrow \pi^*$ |
| | | | 374 (22 500) | $d\pi \rightarrow \pi^*$(py) |
| *trans*-$[RuCl(py)_4(NO)](PF_6)_2$ (**3**) | | 0.31 (100) | 208 (33 500) | $\pi \rightarrow \pi^*$ |
| | | −0.62[d] | 232 (20 000) | $\pi \rightarrow \pi^*$ |
| | | | 258 (15 100) | $d\pi \rightarrow \pi^*$(py) |
| | | | 450 (150)[e] | $d \rightarrow d$, $d\pi \rightarrow \pi^*$(NO) |
| $[RuCl(py)_5]PF_6$ (**4**) | 0.82 (90) | | 204 (30 100) | $\pi \rightarrow \pi^*$ |
| | | | 248 (20 300) | $\pi \rightarrow \pi^*$ |
| | | | 372 (22 500) | $d\pi \rightarrow \pi^*$(py) |
| *trans*-$[RuCl(py)_4(4\text{-Etpy})]PF_6$ (**5**) | 0.78 (95) | | 206 (35 500) | $\pi \rightarrow \pi^*$ |
| | | | 248 (21 400) | $\pi \rightarrow \pi^*$ |
| | | | 374 (25 300) | $d\pi \rightarrow \pi^*$(py) |
| *trans*-$[RuCl(py)_4(PhCN)]PF_6$ (**6**) | 1.04 (95) | | 202 (33 200) | $\pi \rightarrow \pi^*$ |
| | | | 242 (32 000) | $\pi \rightarrow \pi^*$ |
| | | | 352 (27 400) | $d\pi \rightarrow \pi^*$(py) |
| *trans*-$[RuCl(py)_4(pyz)]PF_6$ (**7**) | 0.93 (90) | −1.57 (100) | 202 (33 300) | $\pi \rightarrow \pi^*$ |
| | | | 248 (18 200) | $\pi \rightarrow \pi^*$ |
| | | | 360 (19 100) | $d\pi \rightarrow \pi^*$(py) |
| | | | 448 (7200) | $d\pi \rightarrow \pi^*$(pyz) |
| *trans*-$[RuCl(py)_4(1\text{-MeIm})]PF_6$ (**8**) | 0.63 (90) | | 202 (30 800) | $\pi \rightarrow \pi^*$ |
| | | | 250 (17 600) | $\pi \rightarrow \pi^*$ |
| | | | 380 (19 300) | $d\pi \rightarrow \pi^*$(py) |
| $[\{trans\text{-}RuCl(py)_4\}_2(\mu\text{-pyz})](PF_6)_2$ (**9**) | 1.18 (75)[f] | −1.16 (80)[f] | 204 (58 500) | $\pi \rightarrow \pi^*$ |
| | 0.90 (70)[f] | | 248 (28 900) | $\pi \rightarrow \pi^*$ |
| | | | 270 sh (10 500) | $\pi \rightarrow \pi^*$ |
| | | | 354 (31 000) | $d\pi \rightarrow \pi^*$(py) |
| | | | 570 (23 700) | $d\pi \rightarrow \pi^*$(pyz) |
| *trans*-$[Ru(py)_4(1\text{-MeIm})(MeCN)](PF_6)_2$ (**10**) | 1.22 (80) | | 206 (28 900) | $\pi \rightarrow \pi^*$ |
| | | | 242 (21 700) | $\pi \rightarrow \pi^*$ |
| | | | 344 (20 300) | $d\pi \rightarrow \pi^*$(py) |
| *trans*-$[Ru(py)_4(4\text{-Etpy})(dmabzn)](PF_6)_2$ (**11**) | 1.57 (125) | 1.16 (70) | 202 (45 200) | $\pi \rightarrow \pi^*$ |
| | | | 234 (23 500) | $\pi \rightarrow \pi^*$ |
| | | | 338 (52 800) | $d\pi \rightarrow \pi^*$(py) |

[a] Measured in solutions ca. $10^{-3}$ M in complex and 0.1 M in $[N(C_4H_9\text{-}n)_4]PF_6$ at a Pt disk working electrode (surface area 0.031 $cm^2$) with a scan rate of 200 mV $s^{-1}$. Ferrocene internal reference $E_{1/2}$ = 0.42 V, $\Delta E_p$ = 85 mV. [b] Solutions *ca.* $5 \times 10^{-5}$ M. [c] $E_{pa}$ for an irreversible oxidation process. [d] $E_{pc}$ for an irreversible reduction process. [e] Solution *ca.* $10^{-3}$ M. [f] Ferrocene internal reference $E_{1/2}$ = 0.42 V, $\Delta E_p$ = 70 mV.

disk working electrode (surface area 0.031 $cm^2$) and Pt wire auxiliary electrode by a medium-porosity glass frit. Spectrophotometric grade acetonitrile (Burdick and Jackson) was used as received and tetra-*n*-butylammonium hexafluorophosphate, $[N(n\text{-}C_4H_9)_4]PF_6$, doubly recrystallized from ethanol and dried in vacuo, was used as supporting electrolyte. Solutions containing $10^{-3}$ M analyte (0.1 M electrolyte) were deaerated for 5 min by a vigorous Ar purge. All $E_{1/2}$ values were calculated from $(E_{pa} + E_{pc})/2$ at a scan rate of 200 mV $s^{-1}$ with no correction for junction potentials.

**Synthesis of *trans*-$Ru(NO_2)_2(py)_4$ (1).** To a partial solution of *trans*-$RuCl_2(py)_4$ (1.03 g, 2.11 mmol) in pyridine (100 mL) was added a solution of $NaNO_2$ (0.58 g, 8.41 mmol) in water (30 mL). The mixture was heated at reflux for 15 min. The yellow solution was concentrated on a rotary evaporator until only a few mL of pyridine remained. Water (100 mL) was added and the pale yellow solid collected by filtration, washed with water, and dried: yield 0.84 g, 77%. $\delta_H$ ($CDCl_3$) 8.46 (8 H, d, $H^{2,6} \times 4$), 7.72 (4 H, t, $H^4 \times 4$), 7.17 (8 H, t, $H^{3,5} \times 4$). $\nu(NO_2)$ 1324 (s), 1278 (s) $cm^{-1}$. Anal. Calcd for $C_{20}H_{20}N_6O_4Ru{\cdot}0.5H_2O$: C, 46.33; H, 4.08; N, 16.21. Found: C, 46.04; H, 4.30; N, 16.12.

**Synthesis of *trans*-$Ru(CN)_2(py)_4$ (2).** To a partial solution of *trans*-$RuCl_2(py)_4$ (1.00 g, 2.05 mmol) in pyridine (80 mL) was added a solution of KCN (552 mg, 8.48 mmol) in water (25 mL). The mixture was heated at reflux for 15 min. The golden solution was evaporated to dryness on a rotary evaporator and $CHCl_3$ was added. The inorganic salts were removed by filtration, and the yellow filtrate loaded onto a short column of silica gel. The product was eluted with 20% methanol/dichloromethane into a flask containing pyridine (0.5 mL). The solution was evaporated until only pyridine remained, and diethyl ether was added to afford a yellow precipitate. This was collected by filtration, washed with diethyl ether, and dried: yield 891 mg, 89%. $\delta_H$ ($CDCl_3$) 8.77 (8 H, d, $H^{2,6} \times 4$), 7.59 (4 H, t, $H^4 \times 4$), 7.07 (8 H, t, $H^{3,5} \times 4$). $\nu$(CN) 2062 (s) $cm^{-1}$. Anal. Calcd for $C_{22}H_{20}N_6Ru{\cdot}H_2O$: C, 54.20; H, 4.55; N, 17.24. Found: C, 53.85; H, 4.57; N, 17.13.

**Synthesis of *trans*-$[RuCl(py)_4(NO)](PF_6)_2$ (3).** A solution of **1**·$0.5H_2O$ (1.72 g, 3.32 mmol) in concentrated HCl (sp gr ~1.19, 40 mL) was heated at reflux for 30 min. The orange solution was cooled to room temperature and the addition of aqueous $NH_4PF_6$ afforded an orange precipitate. This was collected by filtration, washed with water, and dried: yield 2.19 g, 85%. $\delta_H$ ($CD_3COCD_3$) 8.80 (8 H, d, $H^{2,6} \times 4$), 8.41 (4 H, t, $H^4 \times 4$), 7.84 (8 H, t, $H^{3,5} \times 4$). $\nu$(NO) 1911 (s) $cm^{-1}$. Anal. Calcd for $C_{20}H_{20}ClF_{12}N_5OP_2Ru$: C, 31.08; H, 2.61; N, 9.06. Found: C, 30.82; H, 2.54; N, 8.96. (Note: the addition of further aqueous $NH_4PF_6$ to the golden filtrate yielded a further 286 mg of product which was estimated by $^1H$ NMR to contain *ca.* 98% **3**.)

**Synthesis of $[RuCl(py)_5]PF_6$ (4).** A solution of **3** (500 mg, 0.647 mmol) and $NaN_3$ (44 mg, 0.677 mmol) in acetone (6 mL) was stirred at room temperature for 1 h. Pyridine (1 mL) was added and the solution stirred for a further 30 min. The acetone was evaporated, and the addition of aqueous $NH_4PF_6$ afforded a yellow precipitate. This was collected by filtration, washed with water, and dried. Purification was effected by column chromatography collecting the major yellow band. The product was then recrystallized from DMF/diethyl ether to

afford a golden solid: yield 307 mg, 70%. $\delta_H$ ($CD_2Cl_2$) 8.29−8.23 (10 H, c m, $H^{2,6}$ × 5), 7.88−7.77 (5 H, c m, $H^4$ × 5), 7.41 (2 H, t, $H^{3,5}$ axial), 7.27 (8 H, t, $H^{3,5}$ × 4). Anal. Calcd for $C_{25}H_{25}ClF_6N_5PRu$: C, 44.35; H, 3.72; N, 10.34. Found: C, 44.29; H, 3.67; N, 10.40.

**Synthesis of *trans*-[RuCl(py)$_4$(4-Etpy)]PF$_6$ (5).** This salt was prepared in similar fashion to **4** by using **3** (200 mg, 0.259 mmol), $NaN_3$ (17.5 mg, 0.269 mmol), acetone (3 mL), and 4-ethylpyridine (0.1 mL) in place of pyridine. The crude product was obtained by evaporation of the acetone followed by the addition of diethyl ether. The golden solid was collected by filtration, washed with diethyl ether, and dried. Column chromatography followed by recrystallization from DMF/diethyl ether afforded golden crystals: yield 137 mg, 75%. $\delta_H$ ($CD_2Cl_2$) 8.27 (8 H, d, $H^{2,6}$ × 4), 8.08 (2 H, d, $J$ = 6.8 Hz, *py*−Et), 7.83 (4 H, t, $H^4$ × 4), 7.30−7.22 (10 H, c m, $H^{3,5}$ × 4, *py*−Et), 2.71 (2 H, q, $J$ = 7.6 Hz, py−*CH*$_2$−Me), 1.25 (3 H, t, $J$ = 7.6 Hz, pyCH$_2$−*Me*). Anal. Calcd for $C_{27}H_{29}ClF_6N_5PRu$: C, 46.00; H, 4.15; N, 9.93. Found: C, 45.86; H, 4.06; N, 9.95.

**Synthesis of *trans*-[RuCl(py)$_4$(PhCN)]PF$_6$ (6).** This salt was prepared and purified in similar fashion to **5** by using **3** (100 mg, 0.129 mmol), $NaN_3$ (9 mg, 0.138 mmol), and benzonitrile (0.1 mL) in place of 4-ethylpyridine. This afforded yellow crystals: yield 56 mg, 62%. $\delta_H$ ($CD_3COCD_3$) 8.56 (8 H, d, $H^{2,6}$ × 4), 8.01−7.94 (6 H, c m, $H^4$ × 4, PhCN(2, 6)), 7.73 (1 H, t, PhCN(4)), 7.59 (2 H, t, PhCN(3, 5)), 7.43 (8 H, t, $H^{3,5}$ × 4). $\nu$(CN) 2210 (m) cm$^{-1}$. Anal. Calcd for $C_{27}H_{25}ClF_6N_5PRu$: C, 46.26; H, 3.59; N, 9.99. Found: C, 46.38; H, 3.63; N, 10.00.

**Synthesis of *trans*-[RuCl(py)$_4$(pyz)]PF$_6$ (7).** A solution of **3** (100 mg, 0.129 mmol) and $NaN_3$ (9 mg, 0.129 mmol) in acetone (3 mL) was stirred at room temperature for 1 h. The resulting solution was added to a stirred solution of pyrazine (220 mg, 2.75 mmol) in acetone (2 mL) and the reaction stirred at room temperature for 30 min. The acetone was evaporated and diethyl ether added. The crude product was collected by filtration, washed with diethyl ether, washed with water, and dried. Purification was effected by recrystallization from DMF/diethyl ether to afford brown crystals: yield 73 mg, 83%. $\delta_H$ ($CD_3SOCD_3$) 8.52 (2 H, d, $J$ = 4.2 Hz, pyz), 8.44 (2 H, d, $J$ = 3.9 Hz, pyz), 8.18 (8 H, d, $H^{2,6}$ × 4), 7.96 (4 H, t, $H^4$ × 4), 7.40 (8 H, t, $H^{3,5}$ × 4). Anal. Calcd for $C_{24}H_{24}ClF_6N_6PRu$: C, 42.52; H, 3.57; N, 12.40. Found: C, 42.78; H, 3.57; N, 12.48.

**Synthesis of *trans*-[RuCl(py)$_4$(1-MeIm)]PF$_6$ (8).** This salt was prepared in similar fashion to **5** by using 1-methylimidazole (0.5 mL) in place of 4-ethylpyridine. Further crude product was obtained by extraction of the aqueous filtrate with dichloromethane (2 × 3 mL). The two portions of crude product were combined and chromatographed by using gradient elution from 2 to 20% (v/v) acetone/dichloromethane, collecting the major golden band. Further purification was effected by two reprecipitations from dichloromethane/diethyl ether: yield 110 mg, 63%. $\delta_H$ ($CD_2Cl_2$) 8.26 (8 H, d, $H^{2,6}$ × 4), 7.79 (4 H, t, $H^4$ × 4), 7.23 (9 H, t, $H^{3,5}$ × 4, Im), 7.07 (1 H, t, $J$ = 1.4 Hz, Im), 6.70 (1 H, t, $J$ = 1.4 Hz, Im), 3.76 (3 H, s, *Me*Im). Anal. Calcd for $C_{24}H_{26}ClF_6N_6PRu$: C, 42.39; H, 3.85; N, 12.36. Found: C, 42.71; H, 3.74; N, 12.04.

**Synthesis of [{*trans*-RuCl(py)$_4$}$_2$($\mu$-pyz)](PF$_6$)$_2$ (9).** This salt was prepared by using three different procedures. *Procedure 1*: A solution of **3** (100 mg, 0.129 mmol) and $NaN_3$ (9 mg, 0.129 mmol) in acetone (2 mL) was stirred at room temperature for 1 h. **7** (88 mg, 0.130 mmol) was added and the solution stirred in the dark for a further 70 h. The dark precipitate was collected by filtration, washed with acetone, and dried to afford 67 mg of crude product. Recrystallization from DMF/diethyl ether followed by reprecipitation from DMF/diethyl ether yielded 57 mg of pure **9** (35%). A further 9 mg of pure product was isolated from the reaction filtrate after standing for a period of 17 d in the dark, giving a cumulative total yield of 40%. $\delta_H$ ($CD_3CN$) 8.16 (16 H, d, $H^{2,6}$ × 8), 7.94 (4 H, s, pyz), 7.89 (8 H, t, $H^4$ × 8), 7.30 (16 H, t, $H^{3,5}$ × 8). Anal. Calcd for $C_{44}H_{44}Cl_2F_{12}N_{10}P_2Ru_2$: C, 41.42; H, 3.48; N, 10.98. Found: C, 41.22; H, 3.87; N, 11.28. *Procedure 2*: This was exactly as procedure 1, except that after addition of **7** the reaction was heated under reflux for 2 h and cooled in iced water before collection of the crude product by filtration. The yield of **9** after recrystallization and reprecipitation was 90 mg, 55%. $\delta_H$ ($CD_3CN$) 8.16 (16 H, d, $H^{2,6}$ × 8), 7.94 (4 H, s, pyz), 7.89 (8 H, t, $H^4$ × 8), 7.30 (16 H, t, $H^{3,5}$ × 8). *Procedure 3*: A solution of **3** (100 mg, 0.129 mmol) and $NaN_3$ (9 mg, 0.129 mmol) in acetone (2 mL) was stirred at room temperature for 1 h. Pyrazine (5.2 mg, 0.065 mmol) was added and the solution stirred in the dark for a further 19 h. The dark precipitate was collected by filtration, washed with acetone and dried to afford 26 mg of crude product. Recrystallization from DMF/diethyl ether followed by reprecipitation yielded 19 mg of pure **9** as a dark purple solid (23%). $\delta_H$ ($CD_3CN$) 8.16 (16 H, d, $H^{2,6}$ × 8), 7.94 (4 H, s, pyz), 7.89 (8 H, t, $H^4$ × 8), 7.30 (16 H, t, $H^{3,5}$ × 8).

**Synthesis of *trans*-[Ru(py)$_4$(1-MeIm)(MeCN)](PF$_6$)$_2$ (10).** A solution of **8** (40 mg, 0.059 mmol) and $TlPF_6$ (51 mg, 0.146 mmol) in acetonitrile (5 mL) and water (3 mL) was stirred at room temperature for 3 d. The addition of aqueous $NH_4PF_6$ afforded a pale yellow precipitate which was collected by filtration, washed with water, and dried. The product was dissolved through the frit in acetone (to leave behind TlCl), precipitated by the addition of diethyl ether, collected by filtration, washed with diethyl ether, and dried to afford a cream-colored solid: yield 45 mg, 92%. $\delta_H$ ($CD_3COCD_3$) 8.36 (8 H, d, $H^{2,6}$ × 4), 8.12 (1 H, s, Im), 8.06 (4 H, t, $H^4$ × 4), 7.49 (9 H, t, $H^{3,5}$ × 4, Im), 7.11 (1 H, t, $J$ = 1.6 Hz, Im), 3.85 (3 H, s, *Me*Im), 2.72 (3 H, s, *Me*CN). $\nu$(CN) 2267 (w) cm$^{-1}$. Anal. Calcd for $C_{26}H_{29}F_{12}N_7P_2Ru$: C, 37.60; H, 3.52; N, 11.80. Found: C, 37.21; H, 3.43; N, 11.57.

**Synthesis of *trans*-[Ru(py)$_4$(4-Etpy)(dmabn)](PF$_6$)$_2$ (11).** A solution of **5** (40 mg, 0.057 mmol), 4-(dimethylamino)benzonitrile (85 mg, 0.581 mmol) and $TlPF_6$ (42 mg, 0.120 mmol) in acetone (6 mL) and water (3 mL) was stirred at room temperature for 3 d. The acetone was evaporated, and addition of aqueous $NH_4PF_6$ afforded a pale yellow precipitate which was collected by filtration, washed with water, and dried. The product was dissolved through the frit in acetone (to leave behind TlCl), precipitated by the addition of diethyl ether, collected by filtration, washed with diethyl ether, and dried. Purification was effected by passage through a short silica gel column using acetone as eluent followed by several recrystallizations from DMF/diethyl ether to remove unreacted **5**. This afforded a pale yellow solid: yield 29 mg, 53%. $\delta_H$ ($CD_3COCD_3$) 8.69 (2 H, d, $J$ = 6.7 Hz, *py*−Et), 8.47 (8 H, d, $H^{2,6}$ × 4), 8.12 (4 H, t, $H^4$ × 4), 7.65 (2 H, d, $J$ = 9.2 Hz, $Me_2N$−$C_6H_4$−CN), 7.61−7.52 (10 H, m, $H^{3,5}$ × 4, *py*−Et), 6.78 (2 H, d, $J$ = 9.2 Hz, $Me_2N$−$C_6H_4$−CN), 3.09 (6 H, s, $Me_2N$), 2.82 (2 H, q, $J$ = 7.7 Hz, py−*CH*$_2$−Me), 1.26 (3 H, t, $J$ = 7.6 Hz, pyCH$_2$-*Me*). $\nu$(CN) 2212 (m) cm$^{-1}$. Anal. Calcd for $C_{36}H_{39}F_{12}N_7P_2Ru{\cdot}H_2O$: C, 44.18; H, 4.22; N, 10.02. Found: C, 43.86; H, 4.21; N, 10.04.

**X-ray Structural Determinations.** Suitable crystals of **6**, **7**, and **9** were grown by slow diffusion of diethyl ether vapor into DMF solutions at room temperature. Crystals selected for diffraction study were as follows: **6**, golden crystal of dimensions 0.20 × 0.20 × 0.45 mm; **7**, brown crystal of dimensions 0.30 × 0.30 × 0.25 mm; **9**, red crystal of dimensions 0.30 × 0.30 × 0.18 mm. Data were collected on a Rigaku AFC6/S diffractometer by using the $\omega$ scan mode for **6** and **7**, and the $\theta/2\theta$ scan mode for **9** with graphite-monochromated Mo K$\alpha$ radiation ($\lambda$ = 0.710 73 Å). Crystallographic data and refinement details are presented in Table 2. Accurate cell constants were obtained from least-squares fits using the following data for **6**, a total of 51 high-angle reflections, 30.00 ≤ 2$\theta$ ≤ 40.00°; for **7**, a total of 54 high-angle reflections, 35.00 ≤ 2$\theta$ ≤ 45.00°; for **9**, a total of 76 high-angle reflections, 30.00 ≤ 2$\theta$ ≤ 40.00°. Of the 2726 unique reflections measured for **6**, 2091 reflections with $I > 2.5\sigma(I)$ were used in the structure solution and subsequent refinement. For **7**, 781 of 1264 unique reflections had $I > 2.5\sigma(I)$, and for **9**, 3810 of 5286 unique reflections had $I > 2.5\sigma(I)$. Final agreement indices obtained with hydrogen atoms placed in their calculated positions were as follows: for **6**, $R$ = 3.7% and $R_w$ = 4.0%; for **7**, $R$ = 4.4% and $R_w$ = 5.2%; for **9**, $R$ = 5.3% and $R_w$ = 6.7%. Weights were estimated from counter statistics.

The crystal of **9** contains 2.0 molecules of DMF per asymmetric unit. Correction was made for absorption in all cases. ORTEP[6] diagrams showing views of the cations are given in Figures 1−3. Selected bond distances are given in Tables 3−5, selected bond angles in Tables 6−8, and final atomic fractional coordinates in Tables 9−11. Anisotropic thermal parameters, hydrogen atomic parameters, and all nonessential bond lengths and angles are provided as supplementary

(6) Johnson, C. K. *ORTEP: A fortran thermal ellipsoid plot program*; Technical Report ORNL-5138; Oak Ridge National Laboratory: Oak Ridge, TN, 1976.

**Table 2.** Crystallographic Data and Refinement Details for *trans*-[RuCl(py)$_4$(PhCN)]PF$_6$ (**6**), *trans*-[RuCl(py)$_4$(pyz)]PF$_6$ (**7**), and [{*trans*-RuCl(py)$_4$}$_2$($\mu$-pyz)](PF$_6$)$_2$·2DMF (**9**·2DMF)

| | *trans*-[RuCl(py)$_4$(PhCN)]PF$_6$ (**6**) | *trans*-[RuCl(py)$_4$(pyz)]PF$_6$ (**7**) | [{*trans*-RuCl(py)$_4$}$_2$($\mu$-pyz)](PF$_6$)$_2$·2DMF (**9**·2DMF) |
|---|---|---|---|
| formula | $C_{27}H_{25}ClF_6N_5PRu$ | $C_{24}H_{24}ClF_6N_6PRu$ | $C_{50}H_{58}Cl_2F_{12}N_{12}O_2P_2Ru_2$ |
| fw | 701.01 | 677.97 | 1422.05 |
| space group | *P4nc*, tetragonal | *P4/ncc*, tetragonal | *C2/c*, monoclinic |
| *a*, Å | 20.191(7) | 10.7624(13) | 19.0564(17) |
| *b*, Å | | | 14.644(3) |
| *c*, Å | 14.557(7) | 24.615(3) | 21.5112(22) |
| $\beta$, deg | | | 91.877(8) |
| *V*, Å$^3$ | 5934(3) | 2851.1(5) | 6007.8(14) |
| *Z* | 8 | 4 | 4 |
| $D_{calc}$, Mg m$^{-3}$ | 1.569 | 1.579 | 1.572 |
| *T*, K | 103 | 298 | 298 |
| $\lambda$ (Mo K$\alpha$), Å | 0.710 73 | 0.710 73 | 0.710 73 |
| *F*(000) | 2807.75 | 1355.87 | 2863.82 |
| $\mu$, mm$^{-1}$ | 0.72 | 0.75 | 0.72 |
| scan type | $\omega$ | $\omega$ | $\theta/2\theta$ |
| $2\theta$ limit, deg | 50 | 50 | 50 |
| *h*, *k*, *l* ranges | 0−24, 0−16, 0−17 | 0−12, 0−9, 0−29 | −22 to 22, 0−17, 0−25 |
| tot. no. of reflcns | 5164 | 2282 | 6280 |
| no. of unique reflcns | 2726 | 1264 | 5286 |
| no. of data with $I > 2.5\,\sigma(I)$ | 2091 | 781 | 3810 |
| $R^a$ | 0.037 | 0.044 | 0.053 |
| $R_w{}^a$ | 0.040 | 0.052 | 0.067 |
| GOF | 1.19 | 1.48 | 1.98 |
| no. of params | 378 | 102 | 325 |
| max res electron dens, e/Å$^3$ | 0.70 | 0.48 | 1.12 |
| min res electron dens, e/Å$^3$ | −0.35 | −0.46 | −0.72 |

$^a$ $R = \Sigma(|F_o| - |F_c|)/\Sigma|F_o|$; $R_w = [\Sigma w(F_o - F_c)^2/\Sigma wF_o^2]^{1/2}$; GOF = $[\Sigma w(F_o - F_c)^2/(\text{no. of reflcns} - \text{no. of params})]^{1/2}$.

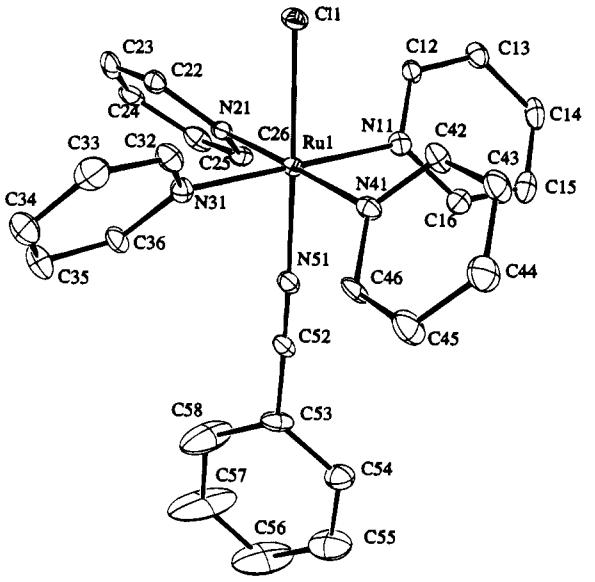


**Figure 1.** Structural representation of the cation of **6**, *trans*-[RuCl(py)$_4$(PhCN)]$^+$, with hydrogen atoms omitted. The thermal ellipsoids correspond to 50% probability.

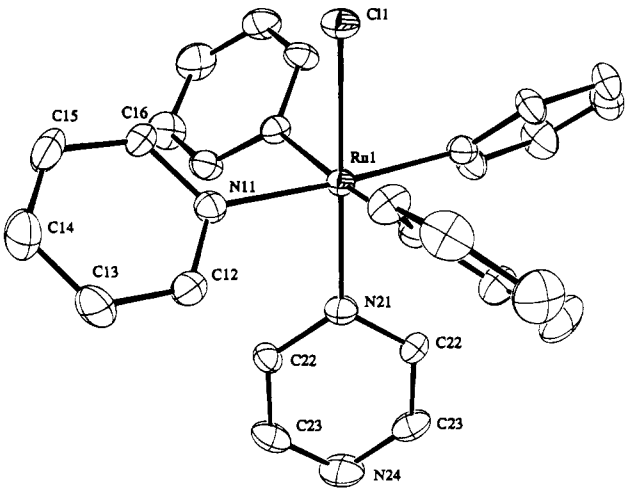


**Figure 2.** Structural representation of the cation of **7**, *trans*-[RuCl(py)$_4$(pyz)]$^+$, with hydrogen atoms omitted. The thermal ellipsoids correspond to 50% probability.

**Table 3.** Selected Bond Distances (Å) for *trans*-[RuCl(py)$_4$(PhCN)]PF$_6$ (**6**)

| | | | |
|---|---|---|---|
| Ru(1)−Cl(1) | 2.3931(22) | Ru(1)−N(41) | 2.076(7) |
| Ru(1)−N(11) | 2.097(7) | Ru(1)−N(51) | 1.989(7) |
| Ru(1)−N(21) | 2.084(7) | N(51)−C(52) | 1.153(11) |
| Ru(1)−N(31) | 2.081(7) | C(52)−C(53) | 1.444(12) |

material. All computations were performed by using the NRCVAX[7] suite of programs. Atomic scattering factors were taken from a standard source[8] and corrected for anomalous dispersion.

## Results and Discussion

**Synthetic Studies.** The complex *trans*-RuCl$_2$(py)$_4$ has been prepared by several different routes.[4,5,9] The two methods of choice are reaction of blue ruthenium(II) chloride solution with pyridine,[4,9b,d,e] and reaction of the precursor RuCl$_2$(DMSO)$_4$ in refluxing pyridine.[5] We found the latter method to be the most convenient, and have obtained yields of up to 90% (based on "RuCl$_3$·3H$_2$O") on a 1.5 g scale by using unpurified RuCl$_2$(DMSO)$_4$. When working on this scale, it is important to heat RuCl$_2$(DMSO)$_4$ in pyridine at reflux for at least 90 min in order

(7) Gabe, E. J.; Le Page, Y.; Charland, J.-P.; Lee, F. L.; White, P. S. *J. Appl. Crystallogr.* **1989**, *22*, 384.
(8) *International Tables for X-ray Crystallography*; Kynoch Press: Birmingham, U.K., 1974; Vol. IV.
(9) (a) Abel, E. W.; Bennett, M. A.; Wilkinson, G. *J. Chem. Soc.* **1959**, 3178. (b) Soucek, J.; Vrestal, J. *Collect. Czech. Chem. Commun.* **1961**, *26*, 1931. (c) Lewis, J.; Mabbs, F. E.; Walton, R. A. *J. Chem. Soc. A* **1967**, 1366. (d) Gilbert, J. D.; Rose, D.; Wilkinson, G. *J. Chem. Soc. A* **1970**, 2765. (e) Nagao, H.; Nishimura, H.; Kitanaka, Y.; Howell, F. S.; Mukaida, M.; Kakihana, H. *Inorg. Chem.* **1990**, *29*, 1693.

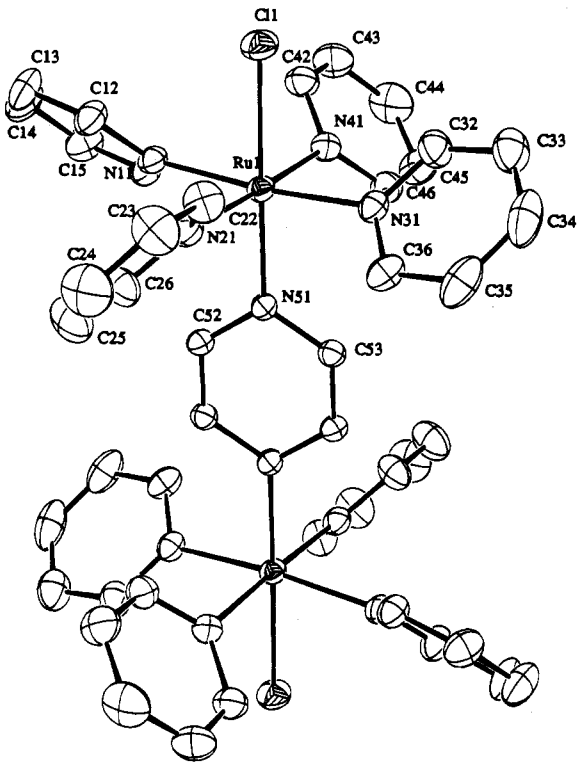


**Figure 3.** Structural representation of the cation of **9**, [{*trans*-RuCl(py)$_4$}$_2$($\mu$-pyz)]$^{2+}$, with hydrogen atoms omitted. The thermal ellipsoids correspond to 50% probability.

**Table 4.** Selected Bond Distances (Å) for *trans*-[RuCl(py)$_4$(pyz)]PF$_6$ (**7**)

| | | | |
|---|---|---|---|
| Ru(1)−Cl(1) | 2.415(3) | N(21)−C(22) | 1.348(13) |
| Ru(1)−N(11) | 2.105(4) | C(22)−C(23) | 1.381(17) |
| Ru(1)−N(21) | 2.091(8) | C(23)−N(24) | 1.319(16) |

**Table 5.** Selected Bond Distances (Å) for [{*trans*-RuCl(py)$_4$}$_2$($\mu$-pyz)](PF$_6$)$_2$·2DMF (**9**·2DMF)

| | | | |
|---|---|---|---|
| Ru(1)−Cl(1) | 2.4092(15) | Ru(1)−N(51) | 2.069(4) |
| Ru(1)−N(11) | 2.096(5) | N(51)−C(52) | 1.344(8) |
| Ru(1)−N(21) | 2.114(5) | N(51)−C(53) | 1.345(7) |
| Ru(1)−N(31) | 2.100(5) | C(52)−C(53)a | 1.370(8) |
| Ru(1)−N(41) | 2.109(5) | | |

**Table 6.** Selected Bond Angles (deg) for *trans*-[RuCl(py)$_4$(PhCN)]PF$_6$ (**6**)

| | | | |
|---|---|---|---|
| Cl(1)−Ru(1)−N(11) | 90.20(19) | N(21)−Ru(1)−N(31) | 91.0(3) |
| Cl(1)−Ru(1)−N(21) | 89.99(18) | N(21)−Ru(1)−N(41) | 178.8(3) |
| Cl(1)−Ru(1)−N(31) | 88.92(20) | N(21)−Ru(1)−N(51) | 88.2(3) |
| Cl(1)−Ru(1)−N(41) | 90.86(20) | N(31)−Ru(1)−N(41) | 88.1(3) |
| Cl(1)−Ru(1)−N(51) | 178.15(19) | N(31)−Ru(1)−N(51) | 90.6(3) |
| N(11)−Ru(1)−N(21) | 90.9(3) | N(41)−Ru(1)−N(51) | 90.9(3) |
| N(11)−Ru(1)−N(31) | 177.9(3) | Ru(1)−N(51)−C(52) | 176.7(7) |
| N(11)−Ru(1)−N(41) | 89.9(3) | N(51)−C(52)−C(53) | 177.8(9) |
| N(11)−Ru(1)−N(51) | 90.3(3) | | |

to convert all of the *cis*-RuCl$_2$(py)$_4$ into its more stable *trans* isomer. Purity of *trans*-RuCl$_2$(py)$_4$ was assessed by elemental analyses and $^1$H NMR spectroscopy.[10]

Conversion of *trans*-RuCl$_2$(py)$_4$ into *trans*-Ru(NO$_2$)$_2$(py)$_4$ (**1**) was previously achieved by reaction with NaNO$_2$ in warm aqueous pyridine for 4 days.[4] We have found that an identical

(10) Anal. Calcd for $C_{20}H_{20}Cl_2N_4Ru$: C, 49.19; H, 4.13; N, 11.47. Found: C, 48.85; H, 3.99; N, 11.46. The presence of any *cis*-RuCl$_2$(py)$_4$ is readily detected by $^1$H NMR spectroscopy. For *trans*-RuCl$_2$(py)$_4$: $\delta_H$ ($CD_2Cl_2$) 8.54 (8 H, d, $H^{2,6}$ × 4), 7.66 (4 H, t, $H^4$ × 4), 7.11 (8 H, t, $H^{3,5}$ × 4). We have found that trace oxidation of *trans*-RuCl$_2$(py)$_4$ in $CDCl_3$ can lead to paramagnetic broadening which does not occur in $CD_2Cl_2$.

**Table 7.** Selected Bond Angles (deg) for *trans*-[RuCl(py)$_4$(pyz)]PF$_6$ (**7**)

| | | | |
|---|---|---|---|
| Cl(1)−Ru(1)−N(11) | 87.83(11) | Ru(1)−N(21)−C(22) | 122.9(6) |
| Cl(1)−Ru(1)−N(21) | 180.0 | N(21)−C(22)−C(23) | 121.8(11) |
| N(11)−Ru(1)−N(11)a | 89.9(3) | C(22)−C(23)−N(24) | 124.0(11) |
| N(11)−Ru(1)−N(11)b | 175.67(16) | C(23)−N(24)−C(23)b | 114.1(10) |
| N(11)−Ru(1)−N(21) | 92.17(11) | | |

**Table 8.** Selected Bond Angles (deg) for [{*trans*-RuCl(py)$_4$}$_2$($\mu$-pyz)](PF$_6$)$_2$·2DMF (**9**·2DMF)

| | | | |
|---|---|---|---|
| Cl(1)−Ru(1)−N(11) | 87.49(13) | N(21)−Ru(1)−N(41) | 178.11(19) |
| Cl(1)−Ru(1)−N(21) | 89.75(14) | N(21)−Ru(1)−N(51) | 90.84(18) |
| Cl(1)−Ru(1)−N(31) | 86.50(14) | N(31)−Ru(1)−N(41) | 91.11(20) |
| Cl(1)−Ru(1)−N(41) | 88.98(14) | N(31)−Ru(1)−N(51) | 92.69(18) |
| Cl(1)−Ru(1)−N(51) | 179.00(14) | N(41)−Ru(1)−N(51) | 90.44(18) |
| N(11)−Ru(1)−N(21) | 89.67(20) | Ru(1)−N(51)−C(52) | 123.9(4) |
| N(11)−Ru(1)−N(31) | 174.00(18) | Ru(1)−N(51)−C(53) | 122.9(4) |
| N(11)−Ru(1)−N(41) | 88.87(20) | N(51)−C(52)−C(53)a | 123.7(5) |
| N(11)−Ru(1)−N(51) | 93.31(18) | N(51)−C(53)−C(52)a | 123.2(5) |
| N(21)−Ru(1)−N(31) | 90.21(20) | C(52)−N(51)−C(53) | 113.1(4) |

product is formed in comparable yield after 15 min at reflux. **1** is shown by IR spectroscopy to be a dinitro complex,[11] but we have observed some evidence[12] for nitro−nitrito linkage isomerism,[13] which has been reported in related *trans*-{Ru(py)$_4$}$^{2+}$ complexes.[14] The reaction of *trans*-RuCl$_2$(py)$_4$ with KCN is entirely analogous to the preparation of **1**, but a different workup is required owing to the partial solubility of *trans*-Ru(CN)$_2$(py)$_4$ (**2**) in water.

The complex *trans*-[RuCl(py)$_4$(NO)]$^{2+}$ was reportedly prepared by warming **1** in ethanol/aqueous HCl, the ethanol being necessary to give good yields of the desired product rather than *trans*-[Ru(OH)(py)$_4$(NO)]$^{2+}$.[4] We have been unable to duplicate this result, isolating only *trans*-[Ru(OH)(py)$_4$(NO)]$^{2+}$ in high yield.[15] A more recent report claimed that *trans*-[RuCl(py)$_4$(NO)]$^{2+}$ is produced quantitatively by heating *trans*-[Ru(OH)(py)$_4$(NO)]$^{2+}$ at 80 °C for 2 h in 6 M aqueous HCl.[16] We have found that the most convenient and reliable method for the preparation of *trans*-[RuCl(py)$_4$(NO)]$^{2+}$ in high yield is to heat **1** for a short period at reflux in concentrated HCl. The reaction to produce *trans*-[Ru(OH)(py)$_4$(NO)]$^{2+}$ occurs instantaneously when **1** is added to the acid, and the solution does not change from golden to orange until reflux is reached.

(11) The strong, sharp bands at 1324 and 1278 cm$^{-1}$ assigned to N-bound nitrite (nitro) in **1** compare with those found in the related complex *trans*-Ru(NO$_2$)$_2$(bpy)$_2$[2] at 1338, 1308, and 1290 cm$^{-1}$. No bands for O-bound nitrite (nitrito) are observed.

(12) In some preparations of **1** the product was found to be contaminated with up to 20% of another pale yellow, diamagnetic complex: $\delta_H$ ($CDCl_3$) 8.85 (8 H, d, $H^{2,6}$ × 4), 8.04 (4 H, t, $H^4$ × 4), 7.62 (8 H, t, $H^{3,5}$ × 4); all signals are shifted downfield by 0.33−0.45 ppm relative to their counterparts in **1**, but show no fine splitting. Contamination of **1** with this impurity has no effect on the yield of the reaction to produce **3**, suggesting that the impurity is a nitrito isomer of **1**.

(13) (a) Adeyemi, S. A.; Miller, F. J.; Meyer, T. J. *Inorg. Chem.* **1972**, *11*, 994. (b) Nakamoto, K. *Infrared and Raman Spectra of Inorganic and Coordination Compounds*, 4th ed.; Wiley: New York, 1986; p 221.

(14) (a) Nagao, H.; Howell, F. S.; Mukaida, M.; Kakihana, H. *J. Chem. Soc., Chem. Commun.* **1987**, 1618. (b) Nishimura, H.; Nagao, H.; Howell, F. S.; Mukaida, M.; Kakihana, H. *Chem. Lett.* **1990**, 133. (c) Satoh, K.; Kuroda, H.; Nagao, H.; Matsubara, K.; Howell, F. S.; Mukaida, M.; Kakihana, H. *Chem. Lett.* **1991**, 529.

(15) To a suspension of *trans*-Ru(NO$_2$)$_2$(py)$_4$·0.5H$_2$O (60 mg, 0.116 mmol) in ethanol (1 mL) was added aqueous HCl (3 M, 1 mL). The solution was heated at 85 °C for 10 min, and then the ethanol was removed on a rotary evaporator. Addition of aqueous NH$_4$PF$_6$ to the golden solution afforded a golden precipitate which was collected by filtration, washed with water, and dried: yield 72 mg, 82%. For *trans*-[Ru(OH)(py)$_4$(NO)](PF$_6$)$_2$: $\delta_H$ ($CD_3SOCD_3$) 8.98 (1 H, OH), 8.50 (8 H, d, $H^{2,6}$ × 4), 8.24 (4 H, t, $H^4$ × 4), 7.69 (8 H, t, $H^{3,5}$ × 4). $\nu$(NO) 1865 (s) cm$^{-1}$. An identical result was obtained by heating at 55 °C for 10 min.

(16) Togano, T.; Kuroda, H.; Nagao, N.; Maekawa, Y.; Nishimura, H.; Howell, F. S.; Mukaida, M. *Inorg. Chim. Acta* **1992**, *196*, 57.

**Table 9.** Final Atomic Fractional Coordinates and Equivalent Isotropic Displacement Coefficients (Å$^2$) for *trans*-[RuCl(py)$_4$(PhCN)]PF$_6$ (**6**)

| atom | *x* | *y* | *z* | $B_{iso}$[a] |
|---|---|---|---|---|
| Ru(1) | 0.68610(3) | 0.76490(3) | 0.82905 | 1.42(3) |
| Cl(1) | 0.75290(10) | 0.78978(10) | 0.69711(15) | 2.04(8) |
| N(11) | 0.6577(3) | 0.6749(3) | 0.7691(5) | 1.8(3) |
| C(12) | 0.6473(4) | 0.6691(4) | 0.6780(6) | 1.8(3) |
| C(13) | 0.6307(4) | 0.6111(4) | 0.6353(6) | 2.2(4) |
| C(14) | 0.6230(4) | 0.5542(4) | 0.6885(7) | 2.8(4) |
| C(15) | 0.6328(4) | 0.5590(4) | 0.7824(7) | 2.6(4) |
| C(16) | 0.6503(4) | 0.6194(4) | 0.8203(8) | 2.1(4) |
| N(21) | 0.6060(3) | 0.8131(3) | 0.7682(4) | 1.6(3) |
| C(22) | 0.6123(4) | 0.8732(4) | 0.7287(6) | 1.9(3) |
| C(23) | 0.5589(5) | 0.9066(4) | 0.6937(6) | 2.5(4) |
| C(24) | 0.4964(5) | 0.8793(5) | 0.6971(6) | 2.7(4) |
| C(25) | 0.4894(4) | 0.8163(5) | 0.7332(6) | 2.5(4) |
| C(26) | 0.5455(4) | 0.7851(4) | 0.7687(6) | 1.8(4) |
| N(31) | 0.7178(3) | 0.8530(3) | 0.8888(5) | 1.9(3) |
| C(32) | 0.7813(4) | 0.8731(4) | 0.8827(6) | 2.2(4) |
| C(33) | 0.8062(5) | 0.9289(5) | 0.9226(7) | 3.2(4) |
| C(34) | 0.7647(6) | 0.9673(5) | 0.9741(7) | 3.4(5) |
| C(35) | 0.6990(5) | 0.9489(5) | 0.9831(7) | 3.3(5) |
| C(36) | 0.6777(4) | 0.8919(4) | 0.9390(6) | 2.2(3) |
| N(41) | 0.7654(3) | 0.7179(3) | 0.8922(5) | 1.8(3) |
| C(42) | 0.8087(4) | 0.6803(4) | 0.8448(7) | 2.4(4) |
| C(43) | 0.8618(5) | 0.6483(5) | 0.8865(7) | 2.7(4) |
| C(44) | 0.8707(5) | 0.6549(5) | 0.9790(8) | 3.6(5) |
| C(45) | 0.8276(5) | 0.6936(5) | 1.0290(7) | 3.2(4) |
| C(46) | 0.7756(4) | 0.7238(5) | 0.9835(6) | 2.2(4) |
| N(51) | 0.6285(3) | 0.7464(3) | 0.9368(5) | 1.9(3) |
| C(52) | 0.5926(4) | 0.7371(4) | 0.9971(6) | 1.8(3) |
| C(53) | 0.5456(4) | 0.7265(5) | 1.0704(6) | 2.6(4) |
| C(54) | 0.5473(5) | 0.6693(5) | 1.1221(7) | 3.1(4) |
| C(55) | 0.5005(6) | 0.6606(6) | 1.1909(8) | 5.0(6) |
| C(56) | 0.4549(7) | 0.7078(10) | 1.2100(11) | 8.3(10) |
| C(57) | 0.4528(8) | 0.7649(11) | 1.1578(12) | 11.7(12) |
| C(58) | 0.5004(7) | 0.7765(8) | 1.0905(11) | 8.0(9) |
| P(1) | 1/2 | 1/2 | 0.9816(4) | 2.79(16) |
| F(11) | 0.5654(3) | 0.5432(3) | 0.9819(4) | 5.3(3) |
| F(12) | 1/2 | 1/2 | 0.8706(7) | 2.7(3) |
| F(13) | 1/2 | 1/2 | 1.0919(7) | 3.0(3) |
| P(2) | 0 | 0 | 0.9380(3) | 1.64(12) |
| F(21) | 0 | 0 | 0.833(4) | 6.3(8) |
| F(22) | −0.0253(7) | −0.0682(8) | 0.9759(13) | 3.6(3) |
| F(23) | −0.0322(5) | −0.0735(5) | 0.9253(9) | 2.72(21) |
| F(24) | −0.0237(9) | −0.0522(10) | 0.8596(13) | 2.6(4) |
| F(25) | −0.0164(16) | −0.0367(12) | 1.0300(19) | 4.9(6) |
| P(3) | 0 | 1/2 | 0.93344(25) | 1.99(13) |
| F(31) | −0.0096(3) | 0.5543(4) | 1.0107(5) | 6.1(4) |
| F(32) | 0.0786(3) | 0.5120(3) | 0.9332(5) | 3.9(3) |
| F(33) | −0.0098(3) | 0.5552(3) | 0.8564(4) | 3.7(3) |

[a] $B_{iso}$ is the mean of the principal axes of the thermal ellipsoid.

A number of attempts at chloride substitution in *trans*-[RuCl(py)$_4$(NO)](PF$_6$)$_2$ (**3**) by using silver(I) or thallium(I) revealed that it is not possible to remove the chloride without decomposition of the complex. This observation is in keeping with the reported short Ru−Cl bond of 2.314(1) Å in the crystal structure of **3**,[17] which is a manifestation of the well-documented *trans*-shortening effect exerted by the strongly $\pi$-accepting nitrosyl ligand *trans* to a good $\sigma$-donor ligand such as chloride.[18]

By using a procedure similar to that reported for the conversion of *cis*-[RuCl(bpy)$_2$(NO)]$^+$ into *cis*-[RuCl(bpy)$_2$(S)]$^+$ (S = acetone or methanol),[13a] we have prepared a number of derivatives in which the nitrosyl ligand in **3** is substituted. Reaction of **3** with 1 equiv of $NaN_3$ in acetone at room temperature causes a darkening of the golden solution, characteristic of the formation of an acetone solvento complex, *trans*-[RuCl(py)$_4$(Me$_2$CO)]$^+$. No attempts have been made to isolate this intermediate since it is likely to be both air and moisture sensitive.[13a] Reaction of the solvento complex *in situ* with a variety of nitrogen ligands (L) proceeds rapidly for L = pyridine

**Table 10.** Final Atomic Fractional Coordinates and Equivalent Isotropic Displacement Coefficients (Å$^2$) for *trans*-[RuCl(py)$_4$(pyz)]PF$_6$ (**7**)

| atom | *x* | *y* | *z* | $B_{iso}$[a] |
|---|---|---|---|---|
| Ru(1) | 3/4 | 3/4 | 0.10599(3) | 2.25(3) |
| Cl(1) | 3/4 | 3/4 | 0.00787(11) | 3.46(8) |
| P(1) | 1/4 | 3/4 | 1/4 | 5.75(21) |
| F(1) | 0.3532(5) | 0.6468 | 1/4 | 8.7(4) |
| F(2) | 0.3210(7) | 0.8197(7) | 0.2040(3) | 12.9(4) |
| N(11) | 0.6144(5) | 0.6093(5) | 0.10275(16) | 2.8(3) |
| C(12) | 0.5078(6) | 0.6151(7) | 0.1311(3) | 3.5(3) |
| C(13) | 0.4149(7) | 0.5277(8) | 0.1264(3) | 4.9(4) |
| C(14) | 0.4305(9) | 0.4297(8) | 0.0924(3) | 5.1(5) |
| C(15) | 0.5371(8) | 0.4215(6) | 0.0629(3) | 4.4(4) |
| C(16) | 0.6265(7) | 0.5128(6) | 0.0682(3) | 3.4(3) |
| N(21) | 3/4 | 3/4 | 0.1909(3) | 3.1(3) |
| C(22) | 0.7100(11) | 0.6527(11) | 0.2207(5) | 2.8(5) |
| C(23) | 0.7095(12) | 0.6555(13) | 0.2768(5) | 4.0(6) |
| N(24) | 3/4 | 3/4 | 0.3059(4) | 5.3(4) |

[a] $B_{iso}$ is the mean of the principal axes of the thermal ellipsoid.

**Table 11.** Final Atomic Fractional Coordinates and Equivalent Isotropic Displacement Coefficients (Å$^2$) for [{*trans*-RuCl(py)$_4$}$_2$($\mu$-pyz)](PF$_6$)$_2$·2DMF (**9**·2DMF)

| atom | *x* | *y* | *z* | $B_{iso}$[a] |
|---|---|---|---|---|
| Ru(1) | 0.29665(3) | 0.18851(3) | 0.152775(20) | 2.775(19) |
| Cl(1) | 0.32608(9) | 0.14486(13) | 0.25841(7) | 4.43(8) |
| N(11) | 0.3864(3) | 0.1175(3) | 0.12642(21) | 3.24(21) |
| C(12) | 0.4473(4) | 0.1271(5) | 0.1594(3) | 4.3(3) |
| C(13) | 0.5057(4) | 0.0752(5) | 0.1495(4) | 5.3(4) |
| C(14) | 0.5029(4) | 0.0092(6) | 0.1061(4) | 6.0(4) |
| C(15) | 0.4419(4) | −0.0025(5) | 0.0703(3) | 4.9(3) |
| C(16) | 0.3855(3) | 0.0520(5) | 0.0818(3) | 3.8(3) |
| N(21) | 0.3577(3) | 0.3080(3) | 0.16469(23) | 3.42(21) |
| C(22) | 0.3555(4) | 0.3565(5) | 0.2178(3) | 4.7(3) |
| C(23) | 0.3923(5) | 0.4346(6) | 0.2271(4) | 6.1(4) |
| C(24) | 0.4338(5) | 0.4660(6) | 0.1829(5) | 7.3(5) |
| C(25) | 0.4374(4) | 0.4174(6) | 0.1271(4) | 6.2(4) |
| C(26) | 0.3998(4) | 0.3397(5) | 0.1210(3) | 4.6(3) |
| N(31) | 0.2096(3) | 0.2558(4) | 0.18881(22) | 3.32(21) |
| C(32) | 0.1694(4) | 0.2150(5) | 0.2296(3) | 4.7(4) |
| C(33) | 0.1162(4) | 0.2566(7) | 0.2595(3) | 5.6(4) |
| C(34) | 0.1040(4) | 0.3469(8) | 0.2476(4) | 6.9(5) |
| C(35) | 0.1442(5) | 0.3926(6) | 0.2068(4) | 6.0(4) |
| C(36) | 0.1967(4) | 0.3440(5) | 0.1774(3) | 4.2(3) |
| N(41) | 0.2385(3) | 0.0668(3) | 0.14219(23) | 3.44(23) |
| C(42) | 0.2660(4) | −0.0128(5) | 0.1606(3) | 4.1(3) |
| C(43) | 0.2350(5) | −0.0940(5) | 0.1483(4) | 5.5(4) |
| C(44) | 0.1713(5) | −0.0974(6) | 0.1164(4) | 6.5(5) |
| C(45) | 0.1415(4) | −0.0159(5) | 0.0988(4) | 5.5(4) |
| C(46) | 0.1754(3) | 0.0630(5) | 0.1123(3) | 4.2(3) |
| N(51) | 0.26954(24) | 0.2257(3) | 0.06238(20) | 2.71(19) |
| C(52) | 0.3138(3) | 0.2222(4) | 0.0151(3) | 2.87(23) |
| C(53) | 0.2049(3) | 0.2548(4) | 0.04496(25) | 2.79(22) |
| P(1) | −0.01053(11) | 0.21338(15) | 0.05086(11) | 5.42(11) |
| F(11) | 0.0438(4) | 0.2611(7) | 0.0930(5) | 16.6(6) |
| F(12) | −0.0695(3) | 0.2743(4) | 0.0779(4) | 11.8(5) |
| F(13) | −0.0602(4) | 0.1704(7) | 0.0057(5) | 17.4(7) |
| F(14) | 0.0513(3) | 0.1545(4) | 0.0243(3) | 8.0(3) |
| F(15) | −0.0251(6) | 0.1427(6) | 0.0983(5) | 17.0(7) |
| F(16) | 0.0075(5) | 0.2875(6) | 0.0045(5) | 16.5(6) |
| O(61) | 0.2446(7) | 0.4569(8) | 0.0335(6) | 16.8(4) |
| C(62) | 0.2816(8) | 0.5256(11) | 0.0531(7) | 11.5(4) |
| N(63) | 0.2430(5) | 0.5962(6) | 0.0669(4) | 7.41(18) |
| C(64) | 0.2808(9) | 0.6756(10) | 0.0912(7) | 13.3(5) |
| C(65) | 0.1709(10) | 0.5957(13) | 0.0636(8) | 16.0(6) |

[a] $B_{iso}$ is the mean of the principal axes of the thermal ellipsoid.

(17) Kimura, T.; Sakurai, T.; Shima, M.; Togano, T.; Mukaida, M.; Nomura, T. *Inorg. Chim. Acta* **1983**, *69*, 135.
(18) (a) Veal, J. T.; Hodgson, D. J. *Inorg. Chem.* **1972**, *11*, 1420. (b) Bottomley, F. *J. Chem. Soc., Dalton Trans.* **1974**, 1600. (c) Bottomley, F. *J. Chem. Soc., Dalton Trans.* **1975**, 2538.

**Scheme 1.** Synthesis of Complexes **1**–**11** (See Text for Abbreviations)

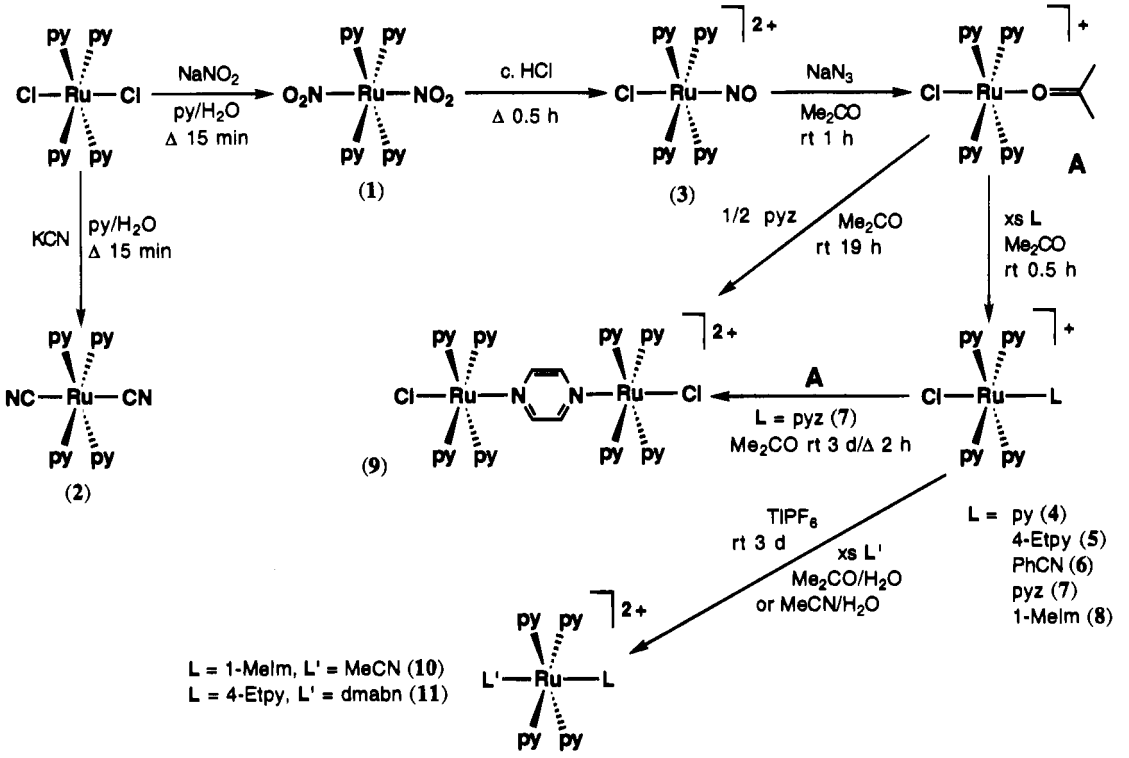


(py), 4-ethylpyridine (4-Etpy), benzonitrile (PhCN), pyrazine (pyz), or 1-methylimidazole (1-MeIm) to give the complexes *trans*-$[RuCl(py)_4(L)]^+$ isolated as the $PF_6^-$ salts **4**–**8** in yields ranging from 62 to 83%. The lower yields are probably due to traces of moisture in the liquid ligands, which were not rigorously dried.

According to electronic *trans* influences, the Ru–Cl bond in the series of complexes in **4**–**8** should weaken, and hence the bond length increase, with increasing $\sigma$-donor power of the ligand L. Hence, the shortest bond should occur when L = benzonitrile, and the longest with L = 1-methylimidazole. This postulate is supported by crystallographic studies (*vide infra*) which show that the Ru–Cl bond lengthens by 0.022 Å when the benzonitrile ligand is replaced by the more basic pyrazine. The chloride in *trans*-$[RuCl(py)_4(1\text{-MeIm})]PF_6$ (**8**) is substituted by using $TlPF_6$ at room temperature in aqueous acetonitrile to yield almost quantitatively the product *trans*-$[Ru(py)_4(1\text{-MeIm})(MeCN)](PF_6)_2$ (**10**). The complex in *trans*-$[RuCl(py)_4(4\text{-Etpy})]PF_6$ (**5**) is less reactive toward chloride substitution, in keeping with the fact that the 4-Etpy ligand is a $\sigma$-donor but also a weak $\pi$-acceptor. Under similar conditions to those used for the conversion of **8** into **10**, **5** was converted into *trans*-$[Ru(py)_4(4\text{-Etpy})(dmabn)](PF_6)_2$ (**11**, dmabn = 4-(dimethylamino)benzonitrile), but a significant quantity of **5** remained unreacted.

The pyrazine-bridged complex $[\{trans\text{-}RuCl(py)_4\}_2(\mu\text{-pyz})](PF_6)_2$ (**9**) was prepared following two routes. Reaction of *trans*-$[RuCl(py)_4(pyz)]PF_6$ (**7**) with a stoichiometric amount of the solvento intermediate, *trans*-$[RuCl(py)_4(Me_2CO)]^+$, proceeds relatively slowly at room temperature, but a reasonable yield of **9** is obtained after a period of 70 h. A little more of the product is obtained if the reaction is allowed to proceed further. The reaction is more efficient if heated, and a considerably improved yield was obtained after 2 h at reflux. A less satisfactory method for the preparation of **9** involves reaction of the solvento intermediate with half an equivalent of pyrazine. The poor solubility of **9** coupled with the formation of large crystals from DMF/diethyl ether facilitates its isolation in pure form. This avoids the necessity for chromatography which could cause light-stimulated decomposition of the complex.

The synthesis of complexes **1**–**11** is shown in Scheme 1.

**UV–Visible Studies.** Absorption spectra for all of the complexes were recorded in acetonitrile, and results are presented in Table 1. All show intense, broad $d\pi(Ru^{II}) \rightarrow \pi^*(py)$ (MLCT) bands in the region 250–400 nm,[19] the energy of which varies with the nature of the axial ligands. Although the maxima occur in the UV region, in **4**, **5**, and **8** the absorptions extend well into the visible region giving rise to intense yellow colors. For example, in **8**, at 450 nm, $\epsilon = 2500$ $M^{-1}$ $cm^{-1}$. The highest energy MLCT (258 nm) is observed for *trans*-$[RuCl(py)_4(NO)](PF_6)_2$ (**3**), and the lowest, for *trans*-$RuCl_2(py)_4$ at 398 nm, with a low-energy shoulder responsible for the dark golden-orange color of this complex. The unusually high apparent extinction for the MLCT band in *trans*-$[Ru(py)_4(4\text{-Etpy})(dmabn)](PF_6)_2$ (**11**) is due to overlap with a $\pi\pi^*$ band of the 4-(dimethylamino)benzonitrile ligand. The free ligand has an absorption at 295 nm in acetonitrile ($\epsilon = 30\,000$ $M^{-1}$ $cm^{-1}$) which shifts to 328 nm ($\epsilon = 39\,000$ $M^{-1}$ $cm^{-1}$) upon complexation to form $[Os(CO)(bpy)_2(dmabn)](PF_6)_2$.[20] The acceptor ability of the nitrile group is increased by complexation to a cationic metal center and this lowers the energy of the $\pi\pi^*$ transition.

The pyrazine complexes show $d\pi(Ru^{II}) \rightarrow \pi^*(pyz)$ MLCT bands in the visible region which have considerably lower extinctions than the $Ru^{II} \rightarrow$ py bands. In *trans*-$[RuCl(py)_4(pyz)]PF_6$ (**7**) the $Ru^{II} \rightarrow$ pyz band occurs at 448 nm. Complexation of a second *trans*-$\{RuCl(py)_4\}^+$ center to the free pyrazine nitrogen in **7** to give **9** produces a marked red shift to 570 nm, together with a 3-fold increase in extinction. This results in

(19) Templeton, J. L. *J. Am. Chem. Soc.* **1979**, *101*, 4906.
(20) Perkins, T. A.; Pourreau, D. B.; Netzel, T. L.; Schanze, K. S. *J. Phys. Chem.* **1989**, *93*, 4511.

part from the higher symmetry of the dimer which leads to a destabilization of the $b_{2g}$ combination of metal orbitals ($xz_1 + xz_2$) by overlap with the filled $b_{2g}$ $\pi$ orbital of the pyrazine.[21] The energy of the $Ru^{II} \rightarrow$ py band in **7** and **9** is almost constant, but there is an extinction increase in the dimer **9**.

The pale orange color of **3** is due to a weak, broad absorption band at 450 nm ($\epsilon$ = 150 $M^{-1}$ $cm^{-1}$, fwhm = 100 nm), most likely resulting from more than one spectroscopically forbidden electronic transition. In the related complex *trans*-$[RuCl(NH_3)_4(NO)]^{2+}$, a similar very weak visible absorption band is observed in water at 440 nm ($\epsilon$ = 17 $M^{-1}$ $cm^{-1}$).[22] This was assigned to a spin-forbidden d−d transition overlapped with a $d\pi(Ru^{II}) \rightarrow \pi^*(NO)$ MLCT absorption.[22] The complex *trans*-$[RuCl(bpy)_2(NO)]^{2+}$ also shows a very weak visible maximum in acetonitrile at 460 nm ($\epsilon$ = 63 $M^{-1}$ $cm^{-1}$).[23] In addition to the MLCT bands, all of the complexes also show high-energy $\pi\pi^*$ bands for the aromatic ligands.

**Electrochemical Studies.** The electrochemical properties of the complexes were studied by cyclic voltammetry in acetonitrile, and results are shown in Table 1. Data for *trans*-$RuCl_2(py)_4$, **1**, and **3** have been previously reported,[9e,14c,24] but are repeated here for purposes of comparison. The complexes *trans*-$RuCl_2(py)_4$ and *trans*-$Ru(CN)_2(py)_4$ (**2**) show reversible $Ru^{III/II}$ oxidation waves, whereas *trans*-$Ru(NO_2)_2(py)_4$ (**1**) displays a completely irreversible oxidative wave, the origin of which has been explained previously.[14c] The potential for **2** is identical to that reported for the related complex *cis*-$Ru(CN)_2(bpy)_2$.[25] For *trans*-$[RuCl(py)_4(NO)](PF_6)_2$ (**3**), the reversible wave at 0.31 V is assigned to a one electron reduction of the $\{Ru(NO)\}^6$ moiety,[26] and the irreversible wave to a second reduction, presumably leading to ligand substitution.[24]

The derivatives, *trans*-$[RuCl(py)_4(L)]^+$ (in **4**−**8**), all show reversible $Ru^{III/II}$ waves, the potentials of which are highly sensitive to the basicity of the ligand L. The pyrazine complex in **7** shows an additional reversible wave corresponding to a one electron reduction of the pyrazine ligand.[27] The disubstituted complex in *trans*-$[Ru(py)_4(1\text{-MeIm})(MeCN)](PF_6)_2$ (**10**) gives a reversible $Ru^{III/II}$ wave, but the oxidative behavior of *trans*-$[Ru(py)_4(4\text{-Etpy})(dmabn)](PF_6)_2$ (**11**) is more complicated. An initial reversible wave is observed at 1.16 V corresponding to one-electron oxidation of the 4-(dimethylamino)benzonitrile ligand. This is unshifted from that reported for the free ligand.[20] Owing to extensive electronic coupling via the nitrile group, ligand oxidation causes an anodic shift of the $Ru^{III/II}$ wave from its expected value of *ca.* 1.3−1.4 V[28] to 1.57 V. The high $\Delta E_p$ value means that this process can be described at best as quasi-reversible.

The pyrazine-bridged complex in **9** shows two reversible $Ru^{III/II}$ waves (Figure 4), indicating a strong intermetallic electronic coupling through the pyz ligand. The first oxidation occurs at a potential almost the same as that for the monometallic **7**, but the second oxidation is markedly shifted, giving

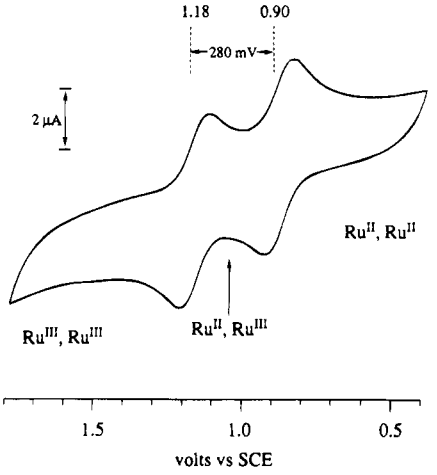


**Figure 4.** Cyclic voltammogram of **9**, $[\{trans\text{-}RuCl(py)_4\}_2(\mu\text{-pyz})](PF_6)_2$ (*ca.* 5 × $10^{-4}$ M), in acetonitrile 0.1 M in $[N(C_4H_9\text{-}n)_4][PF_6]$ at 200 mV $s^{-1}$.

$\Delta E_{1/2}$ = 280 mV. The $\Delta E_p$ values, but not $E_{1/2}$ or $\Delta E_{1/2}$, for these two waves increase with increasing scan rate, suggesting relatively slow electron transfer at the electrode. At 500 mV $s^{-1}$, $\Delta E_p$ values of 135 and 125 mV were obtained for the waves at 1.18 and 0.90 V respectively.

The electrochemical behavior of **9** provides an interesting comparison with that of the related complexes $[(NH_3)_5Ru(pyz)Ru(NH_3)_5]^{4+}$ and *cis*-$[(bpy)_2ClRu(pyz)RuCl(bpy)_2]^{2+}$. These both show two reversible $Ru^{III/II}$ waves, with a $\Delta E_{1/2}$ value of 390 mV for the former[29] and a much smaller $\Delta E_{1/2}$ of 120 mV for the latter.[30] These differences are largely a result of the electronic *trans* influences exerted by the terminal ligands. In the pentaammine complex, the basic $NH_3$ ligands permit a high degree of $d\pi(Ru^{II}) \rightarrow \pi^*(pyz)$ back-bonding which results in a strong electronic communication between the metal centers through the pyz bridge. In the bpy complex, the pyz bridge is *trans* to half of two $\pi$-accepting bpy ligands which compete for back-bonding, thus reducing the available electron density for delocalization through the $\pi^*$ system of the bridge. This leads to a reduced degree of electronic coupling between the Ru centers. In **9**, the *trans* chloride ligands are relatively good $\sigma$-donors, and allow an extent of $d\pi(Ru^{II}) \rightarrow \pi^*(pyz)$ back-donation, and hence intermetallic coupling, which is intermediate between that found in the pentaammine and bpy analogues. The electronic influence of the *cis* $\pi$-acceptor pyridine ligands is less significant in this regard.

The one-electron oxidized form of **9**, $[\{trans\text{-}RuCl(py)_4\}_2(\mu\text{-pyz})]^{3+}$, is of interest for the investigation of its mixed-valence properties. The comparison of $\Delta E_{1/2}$ values indicates that it should exhibit a behavior intermediate between that of the valence-localized (Class II) *cis*-$[(bpy)_2ClRu(pyz)RuCl(bpy)_2]^{3+}$ ion and the Creutz−Taube ion, $[(NH_3)_5Ru(pyz)Ru(NH_3)_5]^{5+}$, which is fully delocalized (Class III) or at the border between Class II and Class III. This will represent a novel addition to the study of intervalence transitions in symmetrically substituted analogues of the Creutz−Taube ion.[31]

Complexation of a second *trans*-$\{RuCl(py)_4\}^+$ moiety to the free pyrazine nitrogen in **7** to give **9** produces a positive

(21) Lauher, J. W. *Inorg. Chim. Acta* **1980**, *39*, 119.
(22) Schreiner, A. F.; Lin, S. W.; Hauser, P. J.; Hopcus, E. A.; Hamm, D. J.; Gunter, J. D. *Inorg. Chem.* **1972**, *11*, 880.
(23) Nagao, H.; Nishimura, H.; Funato, H.; Ichikawa, Y.; Howell, F. S.; Mukaida, M.; Kakihana, H. *Inorg. Chem.* **1989**, *28*, 3955.
(24) Nishimura, H.; Matsuzawa, H.; Togano, T.; Mukaida, M.; Kakihana, H.; Bottomley, F. *J. Chem. Soc., Dalton Trans.* **1990**, 137.
(25) Iwamura, K. M. *Nippon Kagaku Kaishi* **1983**, *10*, 1456.
(26) Callahan, R. W.; Meyer, T. J. *Inorg. Chem.* **1977**, *16*, 574.
(27) Kaim, W. *Angew. Chem., Int. Ed. Engl.* **1983**, *22*, 171.
(28) Calculated by using the Lever electrochemical parameters $E_L$ (V vs NHE) from the following reference: Lever, A. B. P. *Inorg. Chem.* **1990**, *29*, 1271. With values for $E_L$ of py = 0.25, 4-Mepy = 0.23, and PhCN = 0.37, for *trans*-$[Ru(py)_4(4\text{-Mepy})(PhCN)]^{2+}$, $E_{1/2}$ = 1.60 V vs NHE = 1.36 V vs SCE.
(29) (a) Creutz, C.; Taube, H. *J. Am. Chem. Soc.* **1969**, *91*, 3988. (b) *Ibid.* **1973**, *95*, 1086.
(30) Callahan, R. W.; Keene, F. R.; Meyer, T. J.; Salmon, D. J. *J. Am. Chem. Soc.* **1977**, *99*, 1064.
(31) (a) Roberts, J. A.; Hupp, J. T. *Inorg. Chem.* **1992**, *31*, 157. (b) Salaymeh, F.; Berhane, S.; Yusof, R.; de la Rosa, R.; Fung, E. Y.; Matamoros, R.; Lau, K. W.; Zheng, Q.; Kober, E. M.; Curtis, J. C. *Inorg. Chem.* **1993**, *32*, 3895.

shift of 410 mV in the potential for reduction at pyrazine. Pyrazine reduction occurs more readily due to a lowering of the energy of the $\pi^*$ LUMO at pyz upon binding a second $Ru^{II}$ center.

Complex **9** is thermally stable in acetonitrile solution, but exposure to light causes rapid decomposition. Photolysis of an acetonitrile solution of **9** containing 0.1 M $[N(C_4H_9\text{-}n)_4]PF_6$[32] results in formation of a single product with a reversible $Ru^{III/II}$ wave at $E_{1/2} = 0.90$ V. This is likely to be the complex *trans*-$[RuCl(py)_4(CH_3CN)]^+$,[9e] a result consistent with both $^1H$ NMR and UV−visible experiments.[33]

**Structural Studies.** The molecular structures of the cations in **6**, **7**, and **9** are shown in Figures 1−3. These all show the characteristic propeller-like arrangement of the *trans* tetrapyridine core, formed by a tilting of the pyridine rings with respect to the $RuN_4$ plane in order to reduce mutual repulsions. This has been found previously in a number of structures including those of the $Ru^{II}$ salts $[Ru(py)_6](BF_4)_2$,[19] *trans*-$[RuCl(py)_4(NO)](PF_6)_2$,[17] *trans*-$[RuOH(py)_4(NO)](PF_6)_2$,[24] and *trans*-$[RuCl(py)_4(N(OH)CHCOCH_3)]PF_6$,[34] the $Ru^{III}$ salts *trans*-$[RuCl(OH)(py)_4]PF_6$ and *trans*-$[RuCl(OCH_3)(py)_4]ClO_4$,[35] and the $Ru^{IV}$ salt *trans*-$[RuCl(O)(py)_4]ClO_4$.[36] All of the pyridine rings in **6**, **7**, and **9** are essentially planar. In the cation of **6** the pitch of the four pyridine rings varies between 36.7 and 46.7°, giving an average tilt of 40.7°.[37] In the symmetrical cation in **7** the pitch of the propeller is 44.7(3)°.[38] In the bimetallic cation in **9** the pitch of the pyridine rings varies between 41.6 and 47.5°, with an average value of 45.0°.[39]

The average Ru−N(pyridine) bond distances of 2.085(7), 2.105(4), and 2.105(5) Å for **6**, **7**, and **9**, respectively, are similar to those found in related complexes. In **6** the Ru−N(benzonitrile) bond of 1.989(7) Å is considerably shorter than the Ru−N(py) bonds. The nitrogen lone pair in benzonitrile resides in an sp hybrid orbital, and is hence less basic than those of pyridine or pyrazine which exist in $sp^2$ orbitals. However, a greater extent of $d\pi(Ru^{II}) \rightarrow \pi^*$ back-bonding to the nitrile ligand results in formation of a stronger metal-nitrogen bond. In **7** the Ru−N(pyrazine) bond of 2.091(8) Å is only slightly shorter than the Ru−N(py) bonds. The benzonitrile ligand in **6** is approximately linearly bound with Cl(1)−Ru(1)−N(51), Ru(1)−N(51)−C(52) and N(51)−C(52)−C(53) bond angles of 178.15(19), 176.7(7), and 177.8(9)°, respectively. The pyrazine ligand in **7** is disordered, with 50% occupancy in two sites the planes of which lie between, but do not bisect, the N(py)−Ru−N(py) 90° angles.[40] The bimetallic complex in **9** possesses a center of symmetry at the center of the pyrazine bridge, so that the two *trans*-$\{Ru(py)_4\}^{2+}$ centers adopt an eclipsed configuration. The plane of the pyz bridge lies even further from bisecting the N(py)−Ru−N(py) 90° angles than is the case in **7**.[41]

The Ru−Cl bond distances of 2.3931(22) Å in **6**, 2.415(3) Å in **7**, and 2.4092(15) Å in **9** are relatively long owing to the strong $\sigma$-donor capacity of the *trans* ligands. The Ru−Cl bond in **7** is 0.022 Å longer than that in **6** due to the higher basicity of pyrazine. In the parent complex, *trans*-$[RuCl(py)_4(NO)]^{2+}$,[17] the Ru−Cl bond is short at 2.314(1) Å due to the *trans*-shortening effect of the strongly $\pi$-accepting nitrosyl ligand.[18] By contrast, in the derivative *trans*-$[RuCl(py)_4(N(OH)CHCOCH_3)]PF_6$, the high basicity of the $N(OH)CHCOCH_3$ ligand leads to a very long Ru−Cl bond of 2.442(4) Å.[34]

Comparison of the structures of the monomeric complex in **7** and its dimer in **9** is informative. UV−visible and electrochemical measurements (*vide supra*) show that binding of a second *trans*-$\{RuCl(py)_4\}^{2+}$ center to the free pyrazine nitrogen of **7** has a marked effect on the electronic properties of the first $Ru^{II}$ center. It is expected that these differences will also be reflected in the molecular structures of the two complexes. The Ru−Cl and Ru−N(py) bond lengths do not change appreciably between **7** and **9**, but a significant shortening of 0.022 Å can be seen in the Ru−N(pyz) bond distance upon formation of the dimer. This indicates an increased extent of $d\pi(Ru^{II}) \rightarrow \pi^*$(pyz) back-bonding, consistent with the observed strong intermetallic electronic coupling in **9** occurring via the $\pi^*$ system of the pyrazine bridge. The related complexes $[Ru(NH_3)_5(pyz)]^{2+}$[42] and $[(NH_3)_5Ru(pyz)Ru(NH_3)_5]^{4+}$[43] have barely distinguishable Ru−N(pyz) bonds of 2.006(6) and 2.013(3) Å respectively. These are somewhat shorter than those in **7** and **9** due to a greater extent of $d\pi(Ru^{II}) \rightarrow \pi^*$(pyz) back-bonding promoted by the powerful $\sigma$-donor ammine ligands. The only previously reported structure of a bimetallic $\{Ru(py)_4\}^{2+}$ complex is that of the oxalate-bridged *cis* complex, *cis*-$[(py)_4Ru(C_2O_4)Ru(py)_4]^{2+}$.[44]

## Conclusions

Improved methods for the synthesis of the complex *trans*-$Ru(NO_2)_2(py)_4$ and the salt *trans*-$[RuCl(py)_4(NO)](PF_6)_2$ have been developed. Monosubstituted derivatives, *trans*-$[RuCl(py)_4(L)]PF_6$ (L = pyridine, *etc.*), can be readily prepared from *trans*-$[RuCl(py)_4(NO)](PF_6)_2$ by azide-assisted labilization of the electrophilic nitrosyl ligand followed by reaction with ligands L. Replacement of the remaining chloride ligand occurs in the presence of thallium(I) under mild conditions to afford asymmetric derivatives such as *trans*-$[Ru(py)_4(1\text{-MeIm})(MeCN)](PF_6)_2$. Present work is aimed at the exploitation of this chemistry for the synthesis of *trans* chromophore−quencher and ligand-bridged complexes, as an extension of our previous studies with *trans*-$\{Ru(bpy)_2\}^{2+}$ derivatives.

The structurally characterized bimetallic complex $[\{trans\text{-}RuCl(py)_4\}_2(\mu\text{-pyz})]^{2+}$ shows a strong degree of electronic coupling between the two Ru centers which is intermediate between that observed in the previously reported complexes

(32) By using a 150 W Reflector Spot lamp for a period of 1 min.
(33) A photolyzed solution of **9** in $CD_3CN$ gave $\delta_H = 8.58$ (4 H, s, pyz), 8.32 (16 H, d, $H^{2,6} \times 8$), 7.83 (8 H, t, $H^4 \times 8$), 7.26 (16 H, t, $H^{3,5} \times 8$), corresponding to two molecules of *trans*-$[RuCl(py)_4(CD_3CN)]^+$ and one molecule of pyrazine. A photolyzed solution of **9** in $CH_3CN$ gave $\lambda_{max} = 355$, 244 nm.
(34) Bottomley, F.; White, P. S.; Mukaida, M.; Shimura, K.; Kakihana, H. *J. Chem. Soc., Dalton Trans.* **1988**, 2965.
(35) Nagao, H.; Aoyagi, K.; Yukawa, Y.; Howell, F. S.; Mukaida, M.; Kakihana, H. *Bull. Chem. Soc. Jpn.* **1987**, *60*, 3247.
(36) (a) Yukawa, Y.; Aoyagi, K.; Kurihara, M.; Shirai, K.; Shimizu, K.; Mukaida, M.; Takeuchi, T.; Kakihana, H. *Chem. Lett.* **1985**, 283. (b) Aoyagi, K.; Yukawa, Y.; Shimizu, K.; Mukaida, M.; Takeuchi, T.; Kakihana, H. *Bull. Chem. Soc. Jpn.* **1986**, *59*, 1493.
(37) Torsion angles for **6** are as follows: Cl(1)−Ru(1)−N(11)−C(12) = −36.7(4)°; Cl(1)−Ru(1)−N(21)−C(22) = −46.7(4)°; Cl(1)−Ru(1)−N(31)−C(32) = −41.1(4)°; Cl(1)−Ru(1)−N(41)−C(42) = −38.4(4)°.
(38) For **7**, the torsion angle formed by Cl(1)−Ru(1)−N(11)−C(16) is 44.7(3)°.
(39) Torsion angles for **9** are as follows: Cl(1)−Ru(1)−N(11)−C(12) = −44.5(6)°; Cl(1)−Ru(1)−N(21)−C(22) = −41.6(6)°; Cl(1)−Ru(1)−N(31)−C(32) = −46.5(6)°; Cl(1)−Ru(1)−N(41)−C(42) = −47.5(6)°.
(40) For **7**, the torsion angle formed by N(11)−Ru(1)−N(21)−C(22) is 21.6(5)°.
(41) For **9**, the torsion angle formed by N(11)−Ru(1)−N(51)−C(52) is −16.6(5)°.
(42) Gress, M. E.; Creutz, C.; Quicksall, C. O. *Inorg. Chem.* **1981**, *20*, 1522.
(43) Fürholz, U.; Joss, S.; Bürgi, H. B.; Ludi, A. *Inorg. Chem.* **1985**, *24*, 943.
(44) Cheng, P.-T.; Loescher, B. R.; Nyburg, S. C. *Inorg. Chem.* **1971**, *10*, 1275.

$[(NH_3)_5Ru(pyz)Ru(NH_3)_5]^{4+}$ and *cis*-$[(bpy)_2ClRu(pyz)RuCl(bpy)_2]^{2+}$. We are currently investigating the mixed-valence properties of $[\{trans\text{-}RuCl(py)_4\}_2(\mu\text{-}pyz)]^{3+}$, and also the possibilities for derivatization of $[\{trans\text{-}RuCl(py)_4\}_2(\mu\text{-}pyz)]^{2+}$ by chloride substitution. Other work is in progress involving bi- and trimetallic *trans* complexes derived from *trans*-$Ru(CN)_2(py)_4$.

**Acknowledgment.** Support by the U.K. Science and Engineering Research Council under the NATO Postdoctoral Fellowship scheme and also the National Science Foundation (Grant CHE-8806664) is gratefully acknowledged.

**Supplementary Material Available:** Tables of hydrogen atomic parameters, bond distances and angles, and anisotropic thermal parameters for **6** (Tables A–C), **7** (Tables D–F), and **9** (Tables G–I) (20 pages). Ordering information is given on any current masthead page.

IC940862Z